2001

Uncertainties of Monod Kinetic Parameters Nonlinearly Estimated from Batch Experiments

Chongxuan Liu
Pacific Northwest National Laboratory

John M. Zachara
Pacific Northwest National Laboratory, john.zachara@pnl.gov

Environ. Sci. Technol. **2001**, *35,* 133−141

Uncertainties of Monod Kinetic Parameters Nonlinearly Estimated from Batch Experiments

CHONGXUAN LIU* AND
JOHN M. ZACHARA
Pacific Northwest National Laboratory, P.O. Box 999, MSIN K8-96, Richland, Washington 99352

Monod kinetic parameters (K_s, μ_{max}, and Y) that are estimated from batch experimental data can have large uncertainties due to linear correlations between them. The degree of correlation and the resulting uncertainties of the Monod parameters are functions of the initial experimental conditions, the values of the parameters, the type and magnitude of measurement errors, and the sampling number. Careful manipulation of experimental conditions can reduce the correlations between Monod parameters allowing for the estimation of Monod kinetic parameters with the lowest degree of uncertainty. By dimensionless analysis, the correlation and relative standard deviations of Monod parameters were found to be functions of a few dimensionless variables involving the initial substrate (S_0) and cell (X_0) concentrations. Quantitative relationships were analyzed between the dimensionless variables and the correlation and the uncertainties of the Monod parameters. This analysis allowed for identification of the optimal experimental conditions for estimating Monod parameters under both no growth and growth conditions coupled with two kinds of measurement errors: those with constant absolute standard deviation and those with constant relative standard deviation. Examples involving the microbial reduction of iron(III) as an electron acceptor are used to illustrate the application of the developed technique.

Introduction

Large variations have been observed in the values of Monod kinetic parameters determined for a given chemical compound or substrate (*1*). There is consensus that three major factors contribute to the observed variability: culture history, kinetic assay procedure, and linear parameter correlation (*1*). Monod parameters estimated from experiments with different culture history and/or kinetic assay procedures can be different because these factors affect the affinity of the microorganism for substrate (*1*−*4*) and the physiological adaptation of cell enzymes (*1*, and references therein). The linear correlation of Monod kinetic parameters (*5, 6*) complicates the estimation of unique values.

The Monod rate expression (*7*) is often used to describe microbial growth and single substrate degradation kinetics. The Monod rate expression has been extended to include cases when electron acceptors and nutrients are also limiting the growth rate (multiple Monod kinetics) (*8*−*10*). The Monod and extended Monod rate expressions have become the basis for modern biogeochemical modeling (*10*−*21*). The accuracy and uncertainties of Monod rate parameters therefore will have an important influence on the modeling results and their interpretation.

The linear correlation of Monod parameters causes two problems in the estimation of unique values: (1) multiple pairs of correlated parameters may give similar fits to the measurement data and (2) parameter estimation will be highly sensitive to the measurement errors. Mathematically, the first problem is one of uniqueness and the second is one of stability. Both are encountered in "inverse" problems where one uses measurement data to inversely estimate parameters or other unknown properties. For the case of Monod kinetics, mathematical problems result from the correlated nature of the involved parameters. The problem has been termed as parameter identifiability (*22*). Previous studies have found that the extent of correlation of the Monod parameters is strongly dependent on the specific experimental conditions, e.g., substrate and cell concentrations (*5, 23*−*25*). This paper will show that the standard deviations of parameter estimates can range from small to large with increasing levels of Monod parameter correlation. We will also demonstrate that manipulation of experimental conditions can reduce the correlation and thus allow for better parameter estimation (*6, 22, 26*).

Parameter estimation procedures for the Monod kinetic expressions (eqs 1 and 2) have received some literature attention. The Monod equations are (*7*)

$$dS/dt = -(\mu_{max}/Y)SX/(K_s + S) \quad (1)$$

$$dX/dt = \mu_{max}SX/(K_s + S) \quad (2)$$

where S is the substrate concentration, X is the active cell concentration, K_s is the half-maximum concentration, μ_{max} is the maximum growth rate, Y is the cell yield with respect to substrate degradation, and t is time. Sensitivity analyses have been used to identify the linear correlation between Monod parameters (K_s, μ_{max}, and Y). In this method, "sensitivity coefficients" are calculated that are partial derivatives of the substrate concentration with respect to the parameters. For example, $\partial S/\partial K_s$, $\partial S/\partial \mu_{max}$, and $\partial S/\partial Y$ in (1) and (2) are computed as a function of time at different initial substrate (S_0) and cell concentrations (X_0) using realistic values of parameters (K_s, μ_{max}, and Y) (*5, 24, 25*). If *a priori* knowledge regarding the values of parameters, K_s, μ_{max}, and Y, is not available, which is often the case, preliminary experiments are necessary. The goal of the sensitivity coefficient analysis is to avoid initial experimental conditions where one sensitivity coefficient is a linear multiple of others (*22, 26*).

Robinson and Tiedje (*5*) used sensitivity analysis to study the effects of the S_0/K_s ratio on Monod parameter correlation and identifiability. By plotting and visually comparing the sensitivity coefficients as a function of time, the authors found that the Monod parameters were strongly correlated at small (=0.02) and also large (= 50) ratios of S_0/K_s but not at S_0/K_s = 4. Ellis et al. (*25*) used the same approach to determine the optimal initial substrate concentration (S_0) for Monod parameter estimation under constant cell concentration, X. They also visually inspected the sensitivity coefficients and found that large S_0/K_s ratios would reduce the correlation. Ellis et al. (*25*) selected $S_0 = K_s$ as an initial concentration because sensitivity coefficients did not appear to correlate when S_0/K_s is larger than 1. The sensitivity analysis approach was also used to investigate the effect of initial cell concentration, X_0, on the parameter identifiability (*24*). By testing

* Corresponding author phone: (509)376-0129; fax: (509)376-3650; e-mail: chongxuan.liu@pnl.gov.

10.1021/es001261b CCC: $20.00
Published on Web 11/10/2000

different values of X_0 and S_0, Wang (*24*) found that the ratio of S_0/X_0 could affect the Monod parameter correlation. The ratio of S_0/X_0 under constant yield (Y) was also found to affect Monod parameter identifiability by Simkins and Alexander (*23*) in their evaluation of various biological models.

The advantage of the sensitivity approach is that it provides a simple way to illustrate the correlation between Monod parameters under different initial conditions. Also, the sensitivity coefficients can be directly used to identify optimal sampling time points. Parameters estimated from the substrate concentrations measured at these optimal sampling points will have the minimum variances or the best reliability (*6, 27*). However, this sampling technique can be impractical because it requires repeat measurements of the substrate concentration at the optimal time points. Instead, experimentalists usually measure substrate degradation with time and estimate parameters by fitting the Monod model to the time-variable data (e.g. refs *5, 25, 28*). With this latter sampling approach, the identification of optimal experimental conditions using sensitivity analysis suffers disadvantages including the following: (1) the visual inspection of time-variant sensitivity coefficients can only provide a qualitative measure of the correlation between parameters and (2) quantitative information does not result regarding the uncertainties of the parameter estimates and how the correlation affects the uncertainties.

In this communication, a statistics-based approach was developed to investigate Monod parameter correlation and the consequent uncertainties of the parameter estimates. Instead of qualitatively comparing sensitivity coefficients to determine Monod parameter correlation, the developed approach uses time-variant sensitivity coefficients, together with measurement errors and sampling numbers, to calculate the correlation coefficients of Monod parameter estimates and their standard deviations. Specifically, we evaluate the correlation coefficients, standard deviations, and confidence regions of Monod parameters as functions of initial conditions (S_0 and X_0), parameters (μ_{max}, K_s, and Y), types and values of measurement errors, and sample numbers. Through these quantitative analyses, optimal experimental conditions are identified for the development of reliable Monod kinetic parameters.

Variances, Correlation Coefficients, and Confidence Region of Parameter Estimates

The parameters in the Monod rate expressions (eqs 1 and 2) can be estimated by nonlinear or linear methods (*6*, and references cited). However, the results of linear parameter estimation are usually unreliable (*5, 29*). Also, it is difficult to calculate correlation coefficients and variances of estimates from linearized forms because of the transformation of data errors and independent and dependent variables (*6, 22, 26*). Consequently, only nonlinear estimation is considered in the remainder of the paper.

For the convenience of discussion, we rewrite Monod rate expressions (eqs 1 and 2) with respect to substrate concentration as follows

$$dS/dt = f(\boldsymbol{\theta}, S, S_0, X_0, t) \quad (3)$$

where $\boldsymbol{\theta}$ is a vector containing parameters K_s, μ_{max}, and Y, and S_0 and X_0 are the initial substrate and cell concentrations, respectively. According to the statistics of nonlinear parameter estimation, the correlation coefficients, variances, and confidence region of estimates for parameters in eq 3 can be calculated from a covariance matrix of estimates (*22, 26*). Using the least squares or the weighted least-squares method to estimate $\boldsymbol{\theta}$ by fitting eq 3 to measurement data, the covariance matrix of the estimates for normally distributed measurement errors has an asymptotical form (*26*)

$$Cov(\boldsymbol{\theta}) = (\mathbf{J}^T\mathbf{V}^{-1}\mathbf{J})^{-1} = (c_{jk}) \quad (4)$$

where $Cov(\boldsymbol{\theta})$ is a covariance matrix of parameter estimates with its elements of c_{jk} (j, k = 1,2,..., L, and L is the total number of parameters to be estimated). Element c_{jk} is a covariance between parameters j and k. $\mathbf{V}^{-1}$ is the inverse of the covariance matrix of the measurement errors (**V**), superscript *T* denotes matrix transpose, and **J** is a sensitivity coefficient matrix

$$\mathbf{J} = \begin{bmatrix} \frac{\partial S_1}{\partial \theta_1} & \cdots & \frac{\partial S_1}{\partial \theta_L} \\ \vdots & \vdots & \vdots \\ \frac{\partial S_n}{\partial \theta_1} & \cdots & \frac{\partial S_n}{\partial \theta_L} \end{bmatrix} \quad (5)$$

where L is the number of parameters and n is the number of samples. The sensitivity coefficients in eq 5 (**J**) are evaluated at sampling times t_i, i = 1, 2, ..., n. The type and values of matrix **V** are usually dependent on measurement errors.

In the following analysis, we adopted two common literature assumptions regarding measurement errors. First, measurements of substrate concentrations are independent of each other (not correlated). Under this assumption, the matrix **V** becomes diagonal. Second, measurement errors are of two types: (1) those containing constant absolute standard deviation [$\mathbf{V} = \sigma_1^2(\text{data})\mathbf{I}$, σ_1(data) is standard deviation of measurement errors and **I** is an identity matrix] and (2) those containing constant relative standard deviation [$\mathbf{V} = \sigma_2^2(\text{data})[S_i^2]$, $[S_i^2]$ is a diagonal matrix, S_i is the calculated substrate concentration at sampling time t_i, i = 1, 2, ..., n, and σ_2(data) is the relative standard deviation of measurement errors]. The first error type is denoted as type I and the second as type II.

In the covariance matrix (eq 4), diagonal element c_{kk} is the variance [standard deviation square, $\sigma^2(\theta_k)$] of the θ_k estimate. The relative standard deviation ($\sigma(\theta_k)/\theta_k$) is used in this paper to gauge the uncertainty of an estimate (*26*).

The correlation coefficient R between parameters j and k can be estimated as $R^2 = c_{jk}/(c_{jj}c_{kk})$. The confidence region volume (CRV) for a set of estimated parameters (θ_k, k = 1, 2, ..., n) is directly proportional to $\det^{1/2}Cov(\boldsymbol{\theta})$, where $\det Cov(\boldsymbol{\theta})$ represents the determinant of the covariance matrix, $Cov(\boldsymbol{\theta})$ (*26*). The relative CRV (=det $1/2Cov(\boldsymbol{\theta})/\prod_{k=1}^{n}\theta_k$) is used to measure the confidence of a set of estimated parameters when they are correlated (*26*). A large relative CRV means that the set of estimated parameters has large uncertainty.

Numerical Experiments

The evaluation of the covariance matrix (*4*) requires calculations of substrate concentration (S) and sensitivity coefficients ($\partial S/\partial\theta_k$) as a function of time from the Monod model (eqs 1 and 2). Such calculations are more conveniently made with the integral form of the Monod kinetic relationship (*5, 28*):

$$(YK_s + YS_0 + X_0)\ln((Y(S_0 - S) + X_0)/X_0) - YK_s\ln(S/S_0) = \mu_{max}(YS_0 + X_0)t \quad (6)$$

When the cell concentration remains constant through the experiment (no growth), the Monod rate expression has the same form as the Mechalis-Menton rate expression

$$dS/dt = -V_mS/(K_s + S) \quad (7)$$

where $V_m = (\mu_{max}/Y)X_0$ in (1). The K_s in the Michaelis−Menton equation is termed the half- saturation constant. The integral

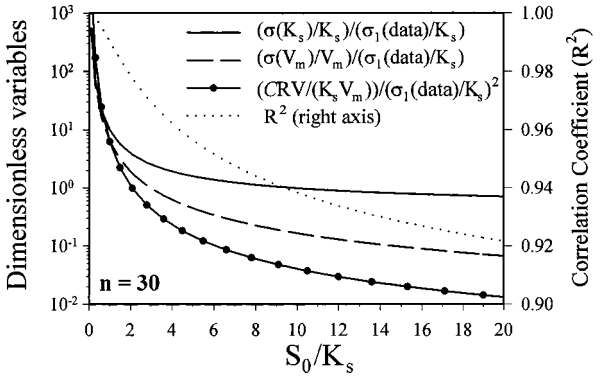

FIGURE 1. The correlation coefficients and standard deviations of estimated Monod kinetic parameters under no growth conditions with type I error. $\sigma(K_s)/K_s$ and $\sigma(V_m)/V_m$ are the relative standard deviations of the K_s and V_m estimates, respectively. $CRV/(K_sV_m)$ and R are the relative confidence region volume and the linear correlation coefficients of the K_s and V_m estimates, respectively. $\sigma_1(data)/K_s$ is the dimensionless measurement precision, and n is the sample number. The correlation coefficient, the relative standard deviations, and the confidence region volume decreased with S_0/K_s.

form of (7) is

$$K_s \ln(S_0/S) + (S_0 - S) = V_m t \quad (8)$$

Kinetic equations 6 (growth) and 8 (no growth) are widely used in bio- and environmental engineering to describe microorganism activities (*28, 30*).

For any specific set of initial substrate and cell concentrations, the substrate concentration (S) and the sensitivity coefficients (5) can be evaluated at sampling time t_i (i = 1,...,n) using either (6) or (8). The covariance matrix can then be computed after coupling the sensitivity coefficients with measurement precision (σ_1(data) or σ_2(data)).

To compare cases with different sets of parameters and initial substrate and cell concentrations, a hypothetical experiment was used where n samples were evenly collected from time 0 to the time when 99% of S_0 was degraded. Analytical formulas were derived for this sampling scheme to evaluate the relative standard deviations, the correlation coefficients, and the relative confidence region volume of the Monod parameter estimates (eg., K_s, μ_{max}, and Y). Cases with no growth and growth coupled with 2 types of measurement errors were considered (see Supporting Information). As we show in the Supporting Information, the correlation coefficients of the Monod parameters are only a function of dimensionless variables: S_0/K_s for no growth and S_0/K_s and X_0/YK_s for growth cases. The relative standard deviation and relative confidence region volume are functions of S_0/K_s and X_0/YK_s (for growth only) and are proportional to dimensionless measurement precision [σ_1(data)/K_s and σ_2(data) for type I and II errors, respectively].

The importance of the dimensionless variables, S_0/K_s and X_0/YK_s [= (X_0/YS_0) x (S_0/K_s)] to the estimation of the Monod parameters can be qualitatively appreciated with equations 1 or 7. When S_0/K_s is small ($S_0 \ll K_s$), S in the denominator of eq 1 or 7 can be neglected, and the equations become first order with respect to substrate concentration, with lumped first-order coefficients of μ_{max}/YK_s for (1) or V_m/K_s for (7). While these lumped parameters can be reliably estimated from experimental data, separation of μ_{max}, Y, and K_s or V_m and K_s is difficult. When $X_0 \gg YS_0$ (YS_0 is the maximum potential for new cells (*23*)), cell growth (eq 2) can be neglected and the 3 parameter Monod model degenerates into one with two parameters: K_s and μ_{max}/Y. Under these conditions, the estimation of μ_{max} and Y is problematic.

TABLE 1. $\sigma(K_s)/\sigma_1$ Changes with S_0/K_s and Sampling Number (n)[a]

	S_0/K_s						
n	0.1	0.5	1	2	5	10	15
10	946	49.8	16.6	6.5	2.4	1.21	0.8
20	670	35.7	12	4.79	1.9	1.13	0.86
30	548	29.3	9.86	3.94	1.57	0.96	0.76
40	475	25.4	8.55	3.42	1.37	0.85	0.68
50	425	22.7	7.65	3.06	1.23	0.76	0.61
60	388	20.7	6.99	2.79	1.12	0.7	0.56
70	359	19.2	6.47	2.59	1.04	0.65	0.52
80	336	18	6.06	2.42	0.97	0.61	0.49
90	317	16.9	5.71	2.28	0.92	0.57	0.46
100	301	16.1	5.42	2.17	0.87	0.54	0.44

[a] No growth with type I error.

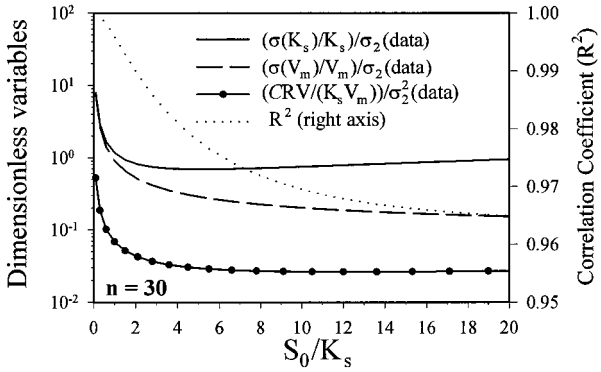

FIGURE 2. The correlation coefficients and the standard deviations of estimated Monod parameters under no growth conditions with type II errors. The symbols are identical to Figure 1 except that σ_2(data) is the relative measurement standard deviation. The lowest relative standard deviation of the K_s estimate (about $0.7\sigma_2$ (data)) was observed at approximately S_0/K_s =5.

In the following section, we will quantitatively examine how the values of S_0/K_s and X_0/YK_s affect the correlation and uncertainties of the estimated Monod parameters. To avoid specific numerical values of dimensionless measurement precision, relative standard deviation and confidence region volume are normalized to dimensionless measurement precision. Consequently, the combined dimensionless variables (relative standard deviations vs dimensionless measurement precision) are only functions of S_0/K_s and X_0/YK_s (growth case) (see Supporting Information). From these analyses, the optimal values of S_0/K_s and X_0/YK_s (growth case) will be identified for the experimental determination of Monod kinetic parameters.

Results

No Growth with Type I Measurement Error. The correlation coefficient and the dimensionless variables related to the relative standard deviations and relative confidence region volume of the estimates K_s and V_m are shown in Figure 1 as functions of S_0/K_s. The values of all dimensionless variables were found to continuously decrease with increasing S_0/K_s (Figure 1). The optimal theoretical laboratory conditions will therefore be at infinitely large S_0/K_s. The relative standard deviation of K_s was always larger than V_m. Therefore, the uncertainty of K_s must be carefully considered. When S_0/K_s was small, the $\sigma(K_s)/\sigma_1(data) = (\sigma(K_s)/K_s)/(\sigma_1(data)/K_s) \gg 1$, indicating that the standard deviations of measurement errors are magnified in the uncertainty of the K_s estimate. For example, $\sigma(K_s) > 500\sigma_1(data)$ when $S_0/K_s < 0.1$. The ratio of $\sigma(K_s)/\sigma_1(data)$ quickly decreased with the increase of S_0/K_s up to 2, and it decreased slowly thereafter. The $\sigma(K_s)/\sigma_1$-

TABLE 2. ($\sigma(K_s)/K_s)/\sigma_2$ Changes with S_0/K_s and Sampling Number (n)[a]

	S_0/K_s						
n	0.1	0.5	1	2	5	10	15
10	13.2	3.15	1.92	1.33	1.06	1.06	1.09
20	9.61	2.31	1.41	0.99	0.82	0.87	0.95
30	7.93	1.91	1.17	0.83	0.69	0.75	0.83
40	6.91	1.66	1.02	0.72	0.61	0.66	0.75
50	6.2	1.49	0.92	0.65	0.55	0.6	0.68
60	5.67	1.37	0.84	0.6	0.5	0.55	0.63
70	5.26	1.27	0.78	0.55	0.47	0.52	0.59
80	4.92	1.19	0.73	0.52	0.44	0.49	0.56
90	4.65	1.12	0.69	0.49	0.41	0.46	0.53
100	4.41	1.06	0.65	0.46	0.39	0.44	0.5

[a] No growth with type II error.

(data) was < 1 when $S_0/K_s > 10$, indicating that uncertainties in the measurement data will not be magnified in the parameter estimates. The relative standard deviations and confidence region volume of the estimates for any fixed S_0/K_s value were directly proportional to a dimensionless ratio, $\sigma_1(\text{data})/K_s$, confirming that with the same measurement precision (σ_1(data)), small K_s values will be more difficult to estimate than large ones (*24*).

The results in Figure 1 were obtained for a sample number of 30. Similar results were also found for different numbers of samples (Table 1). Only values of the dimensionless numbers for $\sigma(K_s)/\sigma_1(\text{data})$ are shown in Table 1, because of the larger uncertainty in the estimate of K_s. Generally, the values of $\sigma(K_s)/\sigma_1(\text{data})$ decrease with increasing sample number and level off at higher sample numbers.

No Growth with Type II Measurement Errors. The uncertainty of the K_s estimate was also larger than that for V_m (Figure 2) for type II measurement errors. However, the values of the relative standard deviations and the confidence region volumes of the K_s and V_m estimates were independent of the magnitude K_s (Figure 2). Thus, only one dimensionless number, S_0/K_s, affected the relative standard deviations of the estimates for a given relative standard deviation of measurement error. Unlike the type I error case (Figure 1), $\sigma(K_s)/K_s$ had its lowest value at $S_0/K_s = 5$. Considering that both $\sigma(V_m)/V_m$ and $CRV/(K_s \times V_m)$ leveled off at $S_0/K_s = 5$ and the relative standard deviation of V_m estimate was always less than K_s, $S_0 = 5K_s$ can be taken as an optimal experimental condition for determining the Monod parameters in eq 7. Table 2 confirmed that this optimal condition was valid for other sample numbers.

Growth with Type I Measurement Errors. The Monod kinetic expression (eqs 1 and 2) has 3 parameters (μ_{max}, K_s, and Y) that require estimation. However, parameter estimation may be divided into two cases considering that the yield value, Y, may be independently estimated from a profile of active cell number vs substrate concentration (*28*). The first case involves estimating μ_{max} and K_s from the substrate concentration profile with known Y, while the second case involves the simultaneous estimation of μ_{max}, K_s, and Y from the substrate concentration profile.

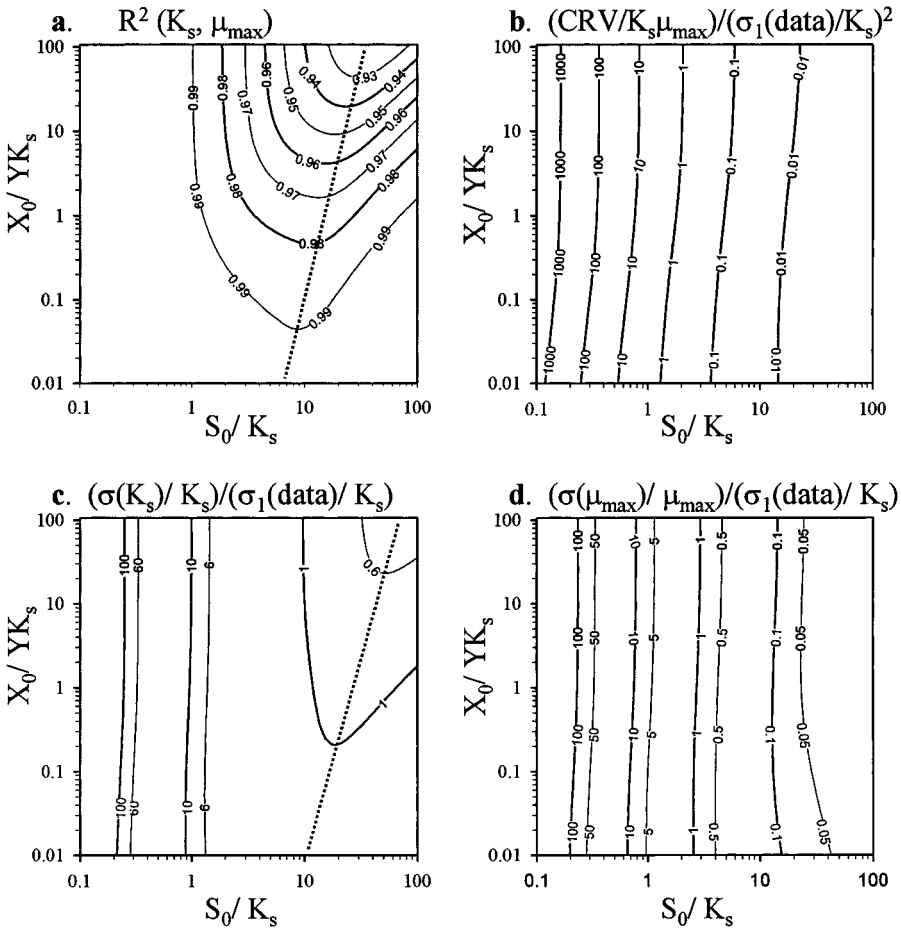

FIGURE 3. The correlation coefficient, the relative standard deviations, and the confidence region volumes of K_s and μ_{max} under growth conditions with type I error and known yield value (Y) (sample number = 30). The relative standard deviation of K_s was always larger than that of μ_{max}. The lowest correlation coefficient (dashed line, Figure 3a) follows $\log(S_0/K_s) = 1.1 + 0.15\log(X_0/YK_s)$. The lowest relative standard deviation of K_s (dashed line, Figure 3c) follows $\log(S_0/K_s) = 1.4 + 0.2\log(X_0/YK_s)$.

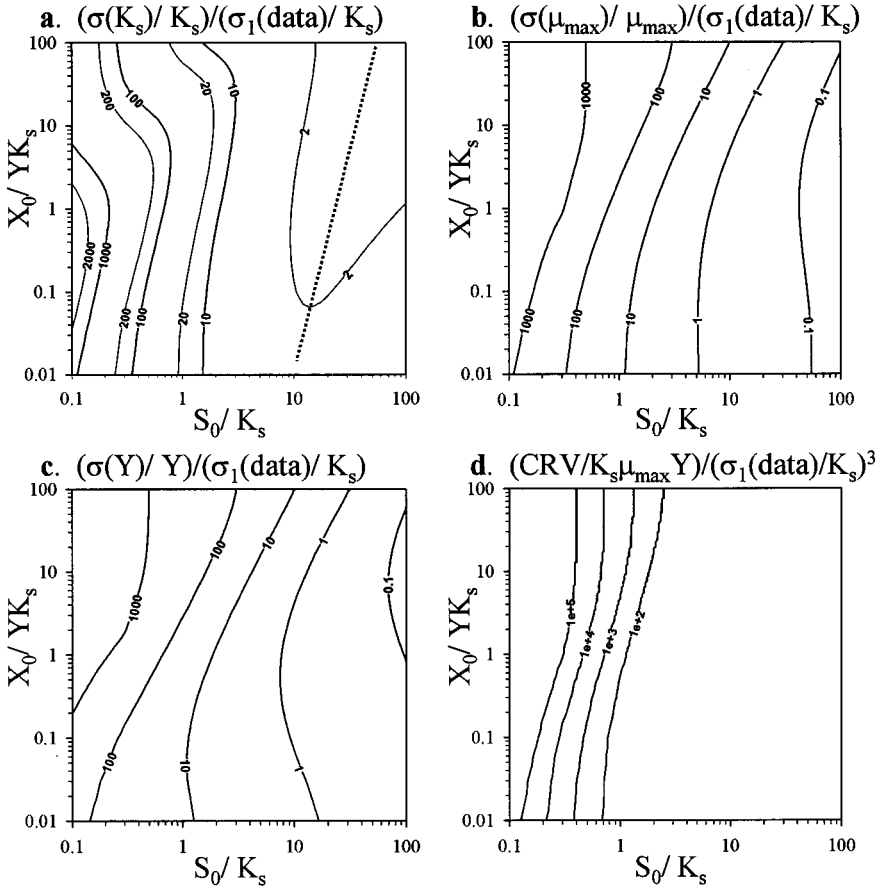

FIGURE 4. The relative standard deviations and confidence region volumes of K_s, μ_{max}, and Y under growth conditions with type I error (sample number = 30). The relative standard deviation of K_s was larger than those of Y and μ_{max} and its lowest value (dashed line) follows $\log(S_0/K_s) = 1.4 + 0.2\log(X_0/YK_s)$.

For cases when Y is independently estimated, the correlation coefficient between K_s and μ_{max} was found to be a function of both X_0 and S_0 (Figure 3) and the lowest correlation coefficient followed the relationship $\log(S_0/K_s) = 1.1 + 0.15 \log(X_0/YK_s)$. The values of the dimensionless variables related to the relative standard deviations and confidence region volume were also found to be influenced primarily by the ratio of S_0/K_s. As under no growth conditions (Figures 1 and 2), the relative standard deviation of K_s was always larger than μ_{max}. The optimal conditions for $\sigma(K_s)/\sigma_1$(data) matched the lowest correlation line and followed $\log(S_0/K_s) = 1.4 + 0.2 \log(X_0/YK_s)$. The relative standard deviations of the K_s and μ_{max} estimates were directly proportional to σ_1(data)/K_s. Thus, it is more difficult to achieve precise small values of K_s than large ones.

When Y was simultaneously estimated with μ_{max} and K_s, the relative standard deviation of K_s was larger than the other parameters when $S_0/K_s > 1$ (Figure 4). The optimal condition for parameter estimation [Figure 4a; $\sigma(K_s)/\sigma_1$(data)] was nearly the same as when Y was independently estimated, $\log(S_0/K_s) = 1.4 + 0.2 \log(X_0/YK_s)$. However, the standard deviations of both K_s and μ_{max} were nearly doubled.

The effects of sample number on the estimation precision were similar to those when no growth occurs. The precision of K_s continuously increased with an increasing sample number (Figure 5 for $S_0/K_s = 25.3$ and $X_0/YK_s = 1.05$) up to a value of approximately 60.

Growth with Type II Measurement Errors. The correlation coefficient, the relative confidence region volume, and the relative standard deviations of K_s and μ_{max} defined an optimal value of S_0/K_s lying between 2 and 6, depending on the value of X_0/YK_s (Figure 6) when Y was independently

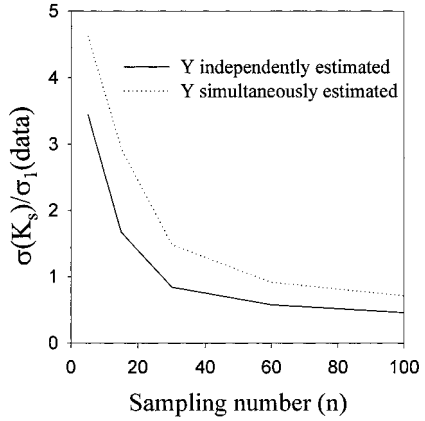

FIGURE 5. The relative standard deviation of K_s changes with sample number (n). $\sigma(K_s)/\sigma_1$(data) decreased rapidly with increasing sample number until $n = 60$ for cases with known yield (Y), and Y simultaneously estimated with K_s and μ_{max}.

estimated. The relative standard deviation of K_s was again larger than that of μ_{max}. The optimal initial conditions were described by $\log(S_0/K_s) = 0.5 + 0.12 \log(X_0/YK_s)$. The standard deviations of both K_s and μ_{max} nearly doubled (Figure 7a,b) when Y was simultaneously estimated with μ_{max} and K_s. A comparison of the relative standard deviations of the three parameters (Figure 7a,b,c) indicated that the optimal regions for estimation of μ_{max}, K_s, and Y were not the same. Therefore, improving the precision of one estimate may decrease the precision of another. The relative standard deviations of μ_{max}, K_s, and Y were usually more than twice the relative standard deviation of the measurement errors. The lowest relative

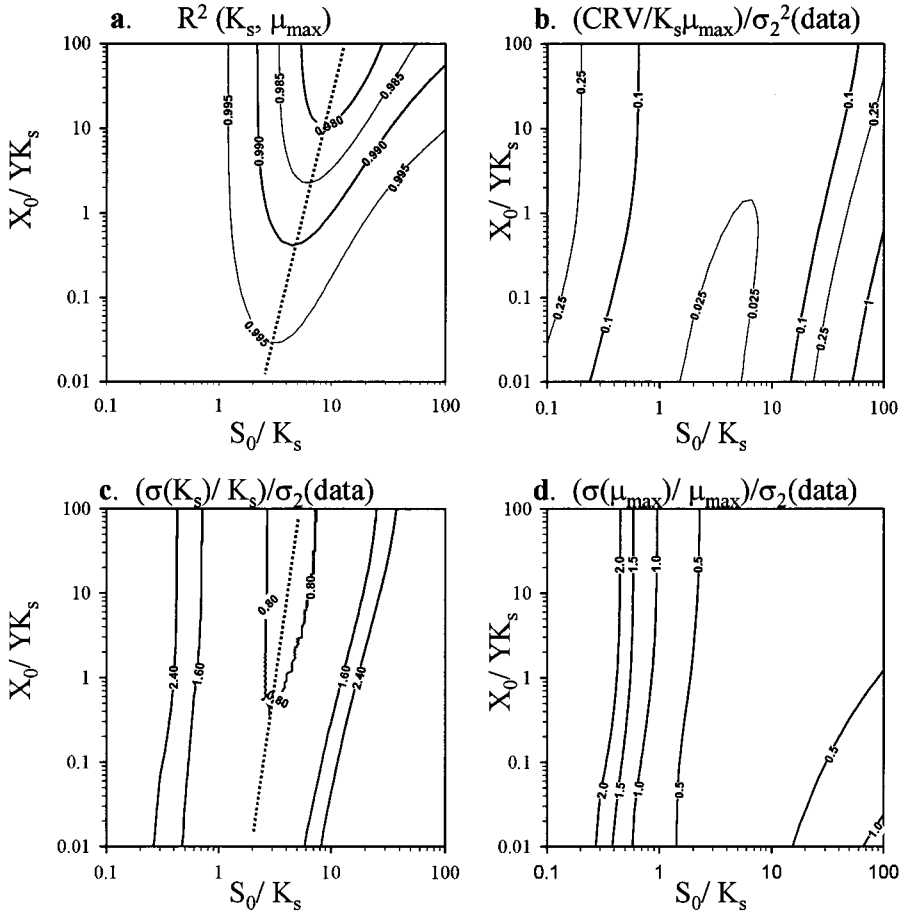

FIGURE 6. The correlation coefficient, the relative standard deviations, and the confidence region volumes of K_s and μ_{max} under growth conditions with type II error and known yield value (Y). The relative standard deviation of K_s was larger than that of μ_{max}. The lowest relative standard deviation of K_s (dashed line, Figure 3b) was within $S_0/K_s = 1-10$ and follows $\log(S_0/K_s) = 1.4 + 0.2\log(X_0/YK_s)$.

standard deviations of these estimates that could be simultaneously obtained were $2.3\sigma_2$(data) for K_s and Y, and $1.0-2.0\sigma_2$(data) for μ_{max}. These follow $\log(S_0/K_s) = 0.85 + 0.23 \log(X_0/YK_s)$, beginning at $X_0/YK_s = 1$.

Discussion

Correlation Coefficient. Correlation between the different Monod parameters has been cited as a cause for the variability of literature reported Monod parameters for a specific compound or substrate (*1*). Our finding that higher correlation coefficient values will result in large standard deviations of parameter estimates supports this conclusion. The quantitative analyses performed herein showed that there was a direct relationship between the correlation coefficients and the uncertainties of the parameter estimates. For example, the standard deviation of K_s under conditions of no growth and type I measurement errors can be expressed as

$$S(K_s) = \sigma_1(\text{data})\left(\sum_{i=1}^{n}\left(\frac{\partial S_i}{\partial K_s}\right)^2 (1 - R^2)\right)^{-1/2} \quad (9)$$

When the parameters K_s and V_m are perfectly correlated, the correlation coefficient (R^2) is 1, and the standard deviation of K_s becomes infinite. Other parameter estimates have similar inverse relationships between the standard deviations of estimates and the correlation coefficients (not shown).

The correlation coefficients (R^2) between the Monod parameters were generally over 0.9 for all cases presented. The significance level of R^2 for 99.5% confidence was about 0.23 (for the 30 sample case), indicating statistical correlation of the Monod parameters for both growth (eqs 1 and 2) and no growth conditions (eq 7). Although, the correlation level can be reduced by adjusting experimental conditions, the correlation between Monod parameters cannot be eliminated. This finding contrasts with that from sensitivity analyses where K_s and V_m under no growth conditions were concluded to show little correlation for $S_0/K_s > 1$ (*25*). Both Figures 1 and 2 indicated that for $S_0/K_s = 1$, the parameters K_s and V_m were highly correlated ($R^2 = 0.99$); even at $S_0/K_s = 20$ the correlation coefficient (R^2) was still above 0.9.

Dimensionless Numbers, S_0/K_s and X_0/YK_s. Both the initial conditions (S_0 and X_0) and the values of the parameters (e.g., μ_{max}, K_s, and Y) can lead to different correlation levels and uncertainties. The effects of each variable on the correlation between the Monod parameters can be estimated by varying one variable and fixing others (*24*). However, our analyses indicated that multivariable effects on the correlation of the Monod parameters could be conveniently described using a few dimensionless numbers. One (S_0/K_s) or two (S_0/K_s and X_0/YK_s) of these numbers were able to describe the correlation of Monod parameters as well as the resulting uncertainties for no growth and growth conditions.

Type and Magnitude of Measurement Errors. The type and values of the measurement errors have significant effects on the correlation of the Monod parameters and also on the uncertainties of the parameter estimates. For both types of errors, the relative standard deviation of the parameter estimates was directly proportional to the dimensionless measurement precision (σ_1(data)/K_s) for type I errors and to σ_2(data) for type II errors. Because the relative standard deviation of the estimates for type I errors was inversely related to K_s, measurement precision must be increased to

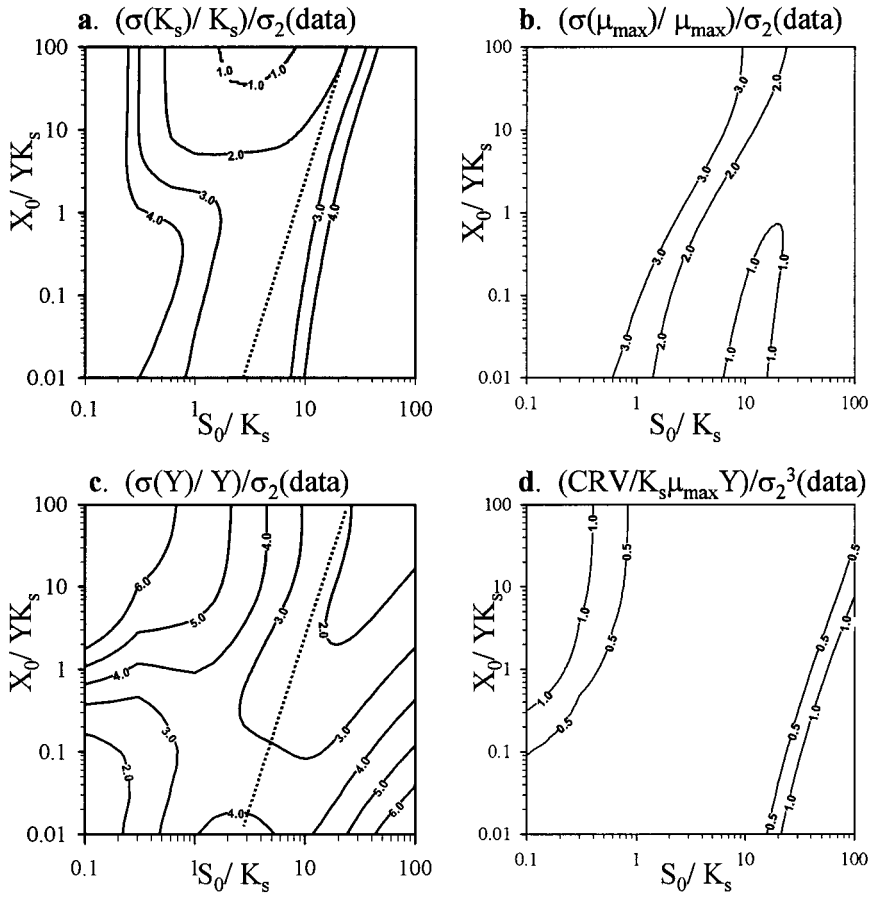

FIGURE 7. The relative standard deviations and the confidence region volumes of K_s, μ_{max}, and Y under growth conditions with type II error. The relative standard deviation of K_s and Y exceeded that of μ_{max} along the dashed line (Figure 7a,c). This dashed line produces the lowest values of the relative standard deviations of K_s and Y (Figure 7a,c) and follows $\log(S_0/K_s) = 0.85 + 0.23\log(X_0/YK_s)$.

maintain the same precision of estimate for small K_s.

The value and type of the standard deviation of the measurement errors can be estimated simultaneously with the Monod parameters under the condition that the measurement errors are randomly distributed (*26*)

$$\sigma^2 = \frac{\mathrm{ER}}{\mathrm{n} - 1} \tag{10}$$

ER is the sum of the least squares errors (for cases with type I errors) or the weighted least squares errors (weighted by the inverse of substrate concentration (1/S) for cases with type II errors) between the measurements and the model calculations. The error type can be determined by plotting the residuals (differences) between the calculated and the measured concentrations as a function of the calculated concentration. When the errors have a constant absolute deviation, the residual plot will show rectangular shape (e.g., inset of Figure 7). In contrast, errors with relative standard deviation produce a triangular plot (the residual increases with increasing concentration). The factors that control error type predominance for biodegradation/transformation type experiments were discussed by Robinson (*6*). Examples of error type determination are provided in the next section.

Sampling Number. The number of samples can also be adjusted to improve the precision of the derived Monod parameters. Normally, the relative standard deviation of the estimated parameter decreases rapidly from small sample number to large. However, the relative standard deviation of the derived parameter will gradually level off when the sample number is large. The improvement in precision is limited when the sample number is increased over 60 for the cases analyzed in this paper.

An Iterative Approach to Monod Parameter Estimation. The optimal experimental conditions for Monod parameter estimation when samples are collected at constantly spaced time intervals are summarized in Table 3. The conditions minimize the mathematical uncertainties of the estimated parameters. The application of Table 3 for optimal experimental design requires *a priori* knowledge of the values of the Monod parameters and the measurement error type. Often, one does not have such information before the start of experiment. Therefore, an iterative or sequential approach is needed where (1) preliminary experiments are performed using guessed S_0 and X_0 values; (2) Monod parameters are estimated using measurement data by least squares or weighted least-squares fitting; (3) the residuals between the Monod model calculations and the measurement data are plotted to check error type and calculate the standard deviation of the measurement errors (previous section); and (4) the values of dimensionless numbers (S_0/K_s, X_0/YK_s) are calculated using the estimated K_s and Y (or independently determined Y) and compared to those in Table 3 to determine whether the experiments were performed under optimal conditions. Steps (1) through (4) are repeated until one obtains reliable estimates of the Monod parameters.

Monod Parameter Estimation for Microbial Iron Reduction

Several examples are now provided of the potential uncertainties and problems associated with the estimation of Monod kinetic parameters. The examples were taken from recent studies of Fe(III) reduction by dissimilatory iron reducing bacteria (*31, 32*). Fe(III) is the electron acceptor and is reduced during microbial respiration. Kinetic rate

TABLE 3. Optimal Experimental Conditions for Monod Parameter Estimation

			growth	
error type[a]	dimensionless no.[b]	no growth	known *Y*	unknown *Y*
I type	S_0/K_s	>5	5−50	10−50
	X_0/YK_s		$\log(S_0/K_s) = 1.4 + 0.2\log(X_0/YK_s)$	$\log(S_0/K_s) = 1.4 + 0.2\log(X_0/YK_s)$
II type	S_0/K_s	5	2−6	1−10
	X_0/YK_s		$\log(S_0/K_s) = 0.5 + 0.12\log(X_0/YK_s)$	$\log(S_0/K_s) = 0.85 + 0.23\log(X_0/YK_s)$

[a] Type I errors exhibit constant absolute standard deviation, and type II errors exhibit constant relative standard deviation. [b] S_0 is the initial substrate concentration, K_s is the half-maximum concentration, X_0 is the initial cell concentration and Y is the cell yield with respect to substrate degradation.

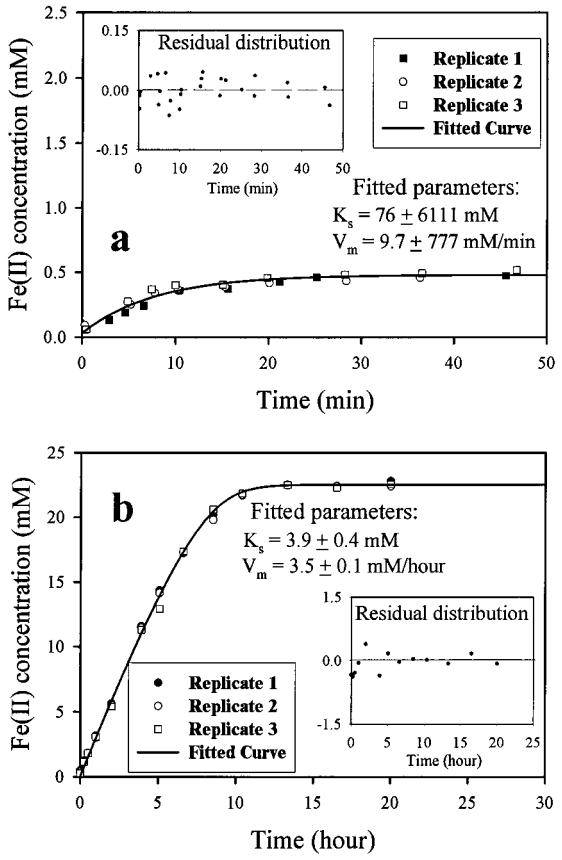

FIGURE 8. Fe(III)-citrate bioreduction by *Shewanella alga* (BrY) under no growth conditions with two initial Fe(III) concentrations: (a) 0.5 mM Fe(III)-citrate and (b) 22.5 mM Fe(III)-citrate. The electron donor (lactate = 30 mM) was in excess.

expressions similar to the Monod relationship have been derived for electron acceptors by assuming: (1) double-substrate limitations on enzyme kinetics (*33, 34*) and (2) an intracellular cofactor response to electron acceptor concentration (*8, 9*). When the substrate concentration is in excess, the kinetic expression for the electron acceptor has the exact mathematical form as the Monod expression (eqs 1 and 2 for growth and eq 7 for no growth conditions) (*8*).

Experimental data and model fitting results for Fe(III)-citrate reduction (0.5 and 22.5 mM) by an iron reducing bacterium, *Shewanella alga* (BrY), under no growth conditions, are shown in Figure 8. Lactate was the electron donor, and its concentration was in excess (*32*). The measurement data in Figure 8a,b were fitted without weights (assuming type I measurement errors) using a modified Levenberg-Marguardt method (*35*). The residuals between the fitted curve and measurement data are plotted in inserts. The fits were excellent in both cases. Residuals were randomly distributed for both initial Fe(III) concentrations (see inserts in Figure 8a,b), suggesting that eq 7 can describe the data

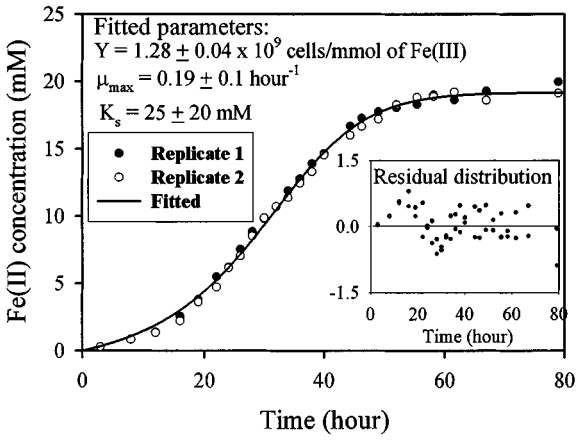

FIGURE 9. Fe(III)-citrate bioreduction by S. *putrefaciens* (CN32) under growth conditions with an initial Fe(III) concentration of 20 mM.

and that the assumption of type I errors used in the least-squares fitting was reasonable. However, the standard deviations of the estimates of K_s and V_m were extremely large when the initial Fe(III) concentration was lower than the K_s estimate (Figure 8a). Obviously, the estimated Monod parameters from Figure 8a are not reliable due to their large standard deviation, despite the excellent fit to the data. Further, the analyses presented in Figure 1 indicated that the correlation between K_s and V_m is almost perfect at small S_0/K_s values. In fact, any pair of large V_m and K_s values with the same ratio of V_m/K_s to those in Figure 8a can give an equivalent fit to the data (Monod model in first-order region). On the other hand, parameter estimates using measurement data with a higher initial Fe(III) concentrations had only small standard deviations and were more reliable (Figure 8b). The ratio of S_0/K_s for latter case is 5.8. As shown in Table 3 and also Figure 1, this ratio is in the range of optimal experimental conditions.

Experimental and model fitting results for Fe(III) bioreduction by another iron reducing bacterium, S. *putrefaciens* CN32, under growth conditions are shown in Figure 9. Here lactate (30 mM) was used as both electron donor and carbon source, and Fe(III)-citrate (20 mM) was the electron acceptor. The initial cell concentration was 1.5×10^9 cells/L. The measurement data were fitted assuming type I measurement errors. An examination of residuals (see insert in Figure 9) indicated that they follow type I characteristics. The residual plot in Figure 9 showed that the model was able to describe the experimental results because there were no obvious trends in residual distribution (*22, 26*). The best estimated parameters were $K_s = 25$ mM, $\mu_{max} = 0.19$ hour^{-1}, and the cell yield value with respect to Fe(III) reduction was 1.28×10^9 cells/mmol of Fe(III).

The growth experiment in Figure 9 was not performed at optimal conditions ($S_0/K_s \approx 1$ and $X_0/YK_s \approx 0.05$) according to Table 3. Therefore, the estimated parameters have

uncertainties, with K_s exhibiting the largest relative standard deviation among the three parameters. The optimal initial conditions for this experiment according to Table 3 are $S_0 =$ 500−2500 mM dependent on X_0. However, the higher initial concentration may increase experiment duration, which, in turn, may lead to other complications, such as carbon and electron donor limitation or microbial physiologic changes that impact yield at later experimental stages (*31*). These complications, if they occur, will require more complex models that further challenge parameter estimation. Consequently, the conditions identified in Table 3 for optimal parameter estimation may need to be balanced against other considerations. Therefore, identification of the best Monod parameters requires careful consideration of the optimal experimental conditions along with other factors that may influence organism physiologic or metabolic status.

Acknowledgments

This research was supported by the Natural and Accelerated Bioremediation Research Program (NABIR), Office of Biological and Environmental Research (OBER), and U.S. Department of Energy (DOE). Pacific Northwest National Laboratory is operated for the U.S. Department of Energy by Battelle Memorial Institute under contract DE AC06-76RLO 1830.

Supporting Information Available

Derives mathematical relationships between dimensionless numbers and statistical variables. This material is available free of charge via the Internet at http://pubs.acs.org.

Literature Cited

(1) Grady, C. P. L. J.; Smets, B. F.; Barbeau, D. S. *Water Res.* **1996**, *30*, 742−748.
(2) Harder, W.; Dijkhuizen, L. *Annu. Rev. Microbiol.* **1983**, *37*, 1−23.
(3) Hofle, M. G. *Appl. Environ. Microbiol.* **1983**, *46*, 1045−1053.
(4) Rutgers, M.; Teixeira De Mattos, M. J.; Postma, P. W.; Van Dam, K. *J. General Microbiol.* **1987**, *133*, 445−451.
(5) Robinson, J. A.; Tiedje, J. M. *Appl. Environ. Microbiol.* **1983**, *45*, 1453−1458.
(6) Robinson, J. A. *Adv. Microbial Ecology* **1985**, *8*, 61−114.
(7) Monod, J. *Annu. Rev. Microbiol.* **1949**, *3*, 371−393.
(8) Bae, W.; Rittmann, B. E. *Biotechnol. Bioeng.* **1996**, *49*, 683−689.
(9) Bae, W.; Rittmann, B. E. *Biotechnol. Bioeng.* **1996**, *49*, 690−699.
(10) Rittmann, B. E.; VanBriesen, J. M. *Rev. Mineral.* **1996**, *34*, 311.
(11) Salvage, K. M.; Yeh, G. T.; Cheng, H. P.; Cheng, J. R. In *Computational Methods in Water Resources XI*; 1996; pp 517−524.
(12) Van Cappellen, P.; Gaillard, J. F.; Rabouille, C. In *Interactions of C, N, P, and S biogeochemical cycles and global change*; Wollast, R., Mackenzie, F. T., Chou, L., Eds.; Springer: Berlin, 1993; pp 401−445.
(13) McNab, W. W.; Narasimhan, T. N. *Water Resources Res.* **1994**, *30*, 2619−2635.
(14) Tebes-Stevens, C.; Valocchi, A. J.; VanBriesen, J. M.; Rittmann, B. E. *J. Hydrol.* **1998**, *209*, 8−26.
(15) Chilakapati, A.; Ginn, T.; Szecsody, J. E. *Water Resources Res.* **1998**, *34*, 1767−1780.
(16) Wood, B. D.; Dawson, C. N.; Szecsody, J. E.; Streile, G. P. *Water Resources Res.* **1994**, *30*, 1833−1845.
(17) Yeh, G. T.; Tripathi, V. S. *Water Resources Res.* **1991**, *27*, 3075−3094.
(18) Viswanathan, H. S.; Robinson, B. A.; Valocchi, A. J.; Triay, I. R. *J. Hydrol.* **1998**, *209*, 251−280.
(19) Essaid, H. I.; Bekins, B. A.; Godsy, E. M.; Warren, E. *Water Resources Res.* **1995**, *31*, 3309−3327.
(20) Clement, T. P.; Sun, Y.; Hooker, B. S.; Petersen, J. N. *Ground Water Monitoring Remediation* **1998**, *Spring*, 79−92.
(21) Steefel, C. I.; Van Cappellen, P. *J. Hydrol.* **1998**, *209*, 1−7.
(22) Beck, J. V.; Arnold, K. J. *Parameter Estimation in Engineering and Science*; John Wiley & Sons: New York, 1977.
(23) Simkins, S.; Alexander, M. *Appl. Environ. Microbiol.* **1984**, *1984*, 1299−1306.
(24) Wang, X. M.S., Clemson University, 1988.
(25) Ellis, T. G.; Barbeau, D. S.; Smets, B. F.; Grady, C. P. L. Jr. *Water Environ. Res.* **1996**, *68*, 917−926.
(26) Bard, Y. *Nonlinear Parameter Estimation*; Academic Press: New York and London, 1974.
(27) Box, G. E. P.; Lucas, H. L. *Biometrika* **1959**, *46*, 77−90.
(28) Gaudy, A. F. J.; Gaudy, E. T. *Microbiology for environmental scientists and engineers*; McGraw-Hill: 1980.
(29) Robinson, J. A.; Characklis, W. G. *Microbial Ecology* **1984**, *10*, 165−178.
(30) Segel, I. H. *Enzyme Kinetics: Behavior and Analysis of Rapid Equilibrium and Steady-State Enzyme Systems*; John Wiley & Sons: 1993.
(31) Liu, C.; Zachara, J. M.; Gorby, Y. A.; Szecsody, J. E.; Brown, C. F. *Environ. Sci. Technol.* **2000**, *Submitted*.
(32) Gorby, Y. A.; Brown, C. F.; Liu, C.; Gray, M. S.; Plymale, A. E.; Li, S.-M.; Fredrickson, J. K.; Wildung, R. E. *unpublished manuscript*.
(33) Bader, F. G. *Biotechnol. Bioeng.* **1978**, *20*, 183−202.
(34) Lehninger, A. L. *Biochemistry*, 2nd ed.; Worth Publisher: New York, 1975.
(35) IMSL. *IMSL Library, Math/Library;* Houston, Texas, 1991.

Received for review May 15, 2000. Revised manuscript received September 21, 2000. Accepted September 28, 2000.

ES001261B